JOURNAL OF SOLID STATE CHEMISTRY **133,** 473–478 (1997)
ARTICLE NO. SC977512

Synthesis and Crystal Structures of Two New Platinum Phosphosilicides, $PtSi_3P_2$ and $PtSi_2P_2$; Electrical Resistivity of $PtSi_3P_2$

Ch. Perrier, M. Kirschen, H. Vincent,[1] U. Gottlieb, B. Chenevier, and R. Madar

ENS de Physique de Grenoble, Laboratoire des Matériaux et du Génie Physique, UMR INPG–CNRS No. 5628, 38402 Saint Martin d'Hères, France

Received June 11, 1997; accepted June 12, 1997

Two phosphosilicides $PtSi_3P_2$ and $PtSi_2P_2$ have been prepared in a tin flux and their crystal structures determined from single crystal X-ray diffraction data. $PtSi_3P_2$ crystallizes in the triclinic space group $P1$, $a = 4.840(1)$ Å, $b = 5.482(1)$ Å, $c = 8.052(1)$ Å, $\alpha = 91.57(1)°$, $\beta = 93.52(1)°$, $\gamma = 108.14(1)°$, $Z = 2$. $PtSi_2P_2$ crystallizes in the monoclinic space group $P2_1$, $a = 6.025(1)$ Å, $b = 9.468(1)$ Å, $c = 11.913(1)$ Å, and $\beta = 102.91(1)°$, $Z = 8$. Final R factors are $R = 0.049$ for the former and $R = 0.040$ for the latter. Pt atoms are octahedrally coordinated by P and Si atoms. P and Si atoms are tetrahedrally surrounded by Pt, Si, and P atoms. In $PtSi_3P_2$ Pt octahedra, connected via edge-sharing, form $Pt_2(Si/P)_{10}$ pairs separated from each other, while $PtSi_2P_2$ exhibits clusters of four edge-sharing octahedra with bonding between clusters via common corners. The behavior of the electrical resistivity of $PtSi_3P_2$ is metallic but with very high values. © 1997 Academic Press

INTRODUCTION

Platinum–silicon chemical interaction has been principally investigated by R. Gohle and K. Schubert (1). Five stable binary silicides have been reported: Pt_3Si, Pt_7Si_3, Pt_2Si, Pt_6Si_5, and PtSi. The last one is used as thin films for Schottky barrier IR detector. Pt_2Si_3 (2) is a metastable phase used as ion beam. In fact, none of the platinum silicide is silicon rich. Among the corresponding phosphides, few compounds have been reported: these include PtP_2, which has the largest phosphorus content (3), and Pt_5P_2.

Few M–Si–P ternary systems (M = transition metal) have been studied. O. G. Folberth *et al.* (4) prepared and studied $CuSi_2P_3$ which is isostructural with ordered chalcopyrite. R. Vogel *et al.* (5) studied the iron–phosphorus–silicon phase diagram and quoted the existence of $FeSi_4P_4$. O. N. Il'Nitskaya *et al.* (6) considered the M–Si–P systems with M = Cr, Mo, W, Re, Co, Ni, and Cu. In the most cases solid solutions are formed, based on binary compounds containing less than 40% nonmetal atoms. However, some high phosphorus–silicon content compounds are quoted, such as $ReSi_4P_4$, $NiSi_3P_4$(7), and $Ni_{3.36}Si_{1.76}P_6$ (8). The latter two were well characterized from single-crystal X-ray diffraction data. No other phases containing transition metals had been reported when we decided no synthesize and characterize such ternary compounds. We have already reported the synthesis and crystal structure of new metal phosphosilicides MSi_xP_y with M = Fe, Co, Ni, Ru, Rh, Pd, Os, Ir, Pt (9, 10). A detailed study of compounds MSi_4P_4 (M = Fe, Ru, Os) (11) and MSi_3P_3 (M = Rh, Ir, or Co) (12–14) has been published. Recently, Jeitschko and collaborators began a systematic study of the same ternary phosphosilicides; an ordered sphalerite-like structure has been proposed for $NiSi_2P_3$ (15). We relate here the study of two other members of this new family of nonmetal-rich transition metal phosphosilicides: $PtSi_3P_2$ and $PtSi_2P_2$.

EXPERIMENTAL

Preparation and Crystal Chemical Characterization

Crystals have been grown by flux method. The used synthesis techniques have been described previously in detail (8). The components mixed in the atomic ratios $M:Si:P = 1:2:2$ and $1:3:3$, with 70% or 80% Sn in weight, were sealed in silica tubes under vacuum, rapidly annealed at 1400 K, and maintained vertically at this temperature for 48 h. Then silica tubes were cooled very slowly (1 K/h) to 1050 K and air quenched. The tin-rich matrix was dissolved in slightly diluted hydrochloric acid. Powder samples were obtained by heating the mixture at 1200 K for 3 weeks. Phosphorus was progressively introduced to control the vapor pressure. Single-phase powders were obtained too, after 1 week only, with iodine as catalyst and transporting agent.

During this study, two kinds of crystals have been obtained under different reaction conditions, but the exact thermodynamic stability range of each kind is not well understood. With the starting molar composition $Pt:Si:P:Sn = 1:2:2:6$ (70% Sn in weight) we have obtained $PtSi_2P_2$ crystals with a very small amount of $PtSi_3P_2$, while

---

[1] To whom correspondence should be addressed.

0022-4596/97 $25.00

with Pt : Si : P : Sn = 2 : 5 : 5 : 13 (82% Sn in weight) we have only prepared $PtSi_3P_2$ crystals. The compositions have been checked by microprobe analysis. For specimens of nominal compositions $PtSi_3P_2$ and $PtSi_2P_2$, the quantitative analysis gives, respectively, in atomic proportion 16.74% Pt, 47.35% Si, 35.91% P, and 19.98% Pt, 40.73% Si, 39.29% P; no tin (detectability limit 0.5%) is revealed inside the crystals. These new compounds have irregular metallic aspects: $PtSi_3P_2$ is more shiny, $PtSi_2P_2$ seems to be particularly sensitive to air. Table 1 gives *hkl* reflections observed from powders using a Guinier camera with Cr$K\alpha_1$ radiation.

Crystal Structure Determination

Most part of the large crystals are polycrystals. Suitable single crystals obtained by cracking larger crystals have been examined with Mo$K\alpha$ radiation using a Buerger precession camera. $PtSi_3P_2$ and $PtSi_2P_2$ have triclinic and monoclinic symmetry, respectively. No systematic extinction is observed for the former, and two space groups are possible: $P1$ and P-1. For the latter, only one extinction rule is observed: $0k0$ reflections with $k = 2n + 1$; the two possible space groups are $P2_1$ and $P2_1/m$.

Two single crystal were then selected for data collection using a four-circle diffractometer. More than 5000 reflections, within the range $3^\circ \leq 2\theta \leq 70^\circ$, have been measured with graphite-monochromated Mo$K\alpha$ radiation. Usual Lorentz-polarization, background, as well as *in situ* absorption corrections, were applied. As the statistical method of Wilson and the nonlinear optical tests exclude any symmetry center, crystal structure determination was carried out using classical methods in the two acentric space groups. The atom kind (Si or P) occupying the nonmetal sites was found by refining the atomic population on each site. For the first time, only one isotropic thermal parameter was applied and refined on the nonmetal sites. Nevertheless, results about the population of these sites have to be considered cautiously because they are correlated with the absorption corrections. After refinement the final R factors are about 0.04 for both crystal structures. Details about crystal data, data collection, and refinement conditions are given in Table 2. Final atomic parameters and interatomic distances between nearest neighbors are given in Tables 3, 4, 5, and 6.

DISCUSSION

All of the transition metal phosphosilicides we have studied, with compositions MSi$_4$P$_4$, MSi$_3$P$_3$, MSi$_3$P$_4$, and here MSi$_2$P$_3$ and MSi$_2$P$_2$, crystallize in different acentric structures. The platinum phosphosilicides related here show many structural similarities with the two first compositions and on the whole with all binary transition metal phosphides MP$_4$, MP$_3$, and MP$_2$. The metal atoms are always octahedrally surrounded by silicon and phosphorus atoms, and all nonmetal atoms are tetrahedrally coordinated by metal or nonmetal atoms; so one observes tetrahedra with zero, one, two, or three Pt atoms at the vertices. In fact,

TABLE 1
Guinier Powder Patterns of $PtSi_3P_2$ and $PtSi_2P_2$

$PtSi_3P_2$						$PtSi_2P_2$					
h	k	l	d_{measured}	$\theta_{\text{obs}} - \theta_{\text{calc}}$	I_{obs}[a]	h	k	l	d_{measured}	$\theta_{\text{obs}} - \theta_{\text{calc}}$	I_{obs}[a]
0	0	1	8.0346	0.004	w	0	1	1	7.3596	0.011	m
0	−1	0	5.2075	0.003	s	0	0	2	5.8282	0.003	vw
1	0	0	4.5935	0.003	s	1	1	0	5.0023	0.012	s
0	−1	1	4.4714	−0.003	s	−1	1	1	4.9603	−0.016	s
−1	1	0	4.1519	0.002	s	0	2	0	4.7490	0.007	w
−1	0	1	4.1218	−0.001	m	0	2	1	4.3957	0.014	m
0	0	2	4.0193	−0.001	s	−1	1	2	4.2135	0.003	s
1	−1	1	3.6476	0.001	m	1	2	0	3.6958	0.010	m
0	−1	2	3.2586	0.001	w	0	1	3	3.5958	0.002	w
1	−1	2	2.8486	−0.003	m	1	1	2	3.4825	0.010	s
1	1	1	2.7502	−0.002	m	1	2	1	3.3895	0.003	vs
0	0	3	2.6792	0.003	w	−1	2	2	3.3398	0.011	w
2	−1	0	2.3982	−0.001	m	0	3	1	3.0551	0.006	s
2	0	1	2.1670	0.001	w	0	2	3	3.0064	0.011	vw
−2	1	2	2.1108	−0.001	m	2	0	0	2.9443	0.004	vw
−2	2	2	1.8661	0.000	m	0	0	4	2.9134	0.003	vs
0	1	4	1.8454	−0.001	s	−2	0	2	2.9134	0.007	vs
−1	3	1	1.7711	0.000	m	−1	2	3	2.8882	0.001	s

[a] Abbreviations: vs, very strong; s, strong; m, medium; w, weak; vw, very weak.

TABLE 2
Crystal Data, Data Collection, and Refinement Parameters

Chemical formula	$PtSi_3P_2$	$PtSi_2P_2$
Crystal system	Triclinic	Monoclinic
Space group	$P1$	$P2_1$
Cell parameters		
a (Å)	4.840(1)	6.025(1)
b (Å)	5.482(1)	9.468(1)
c (Å)	8.052(2)	11.913(1)
α (°)	91.57(1)	
β (°)	93.52(1)	102.91(1)
γ (°)	108.14(1)	
Volume (Å^3)	202.3	662.2
Z	2	8
ρ_{calc} (g cm^{-3})	5.656	6.327
Crystal size (mm)	0.25 × 0.20 × 0.13	0.11 × 0.10 × 0.10
Color	Shiny black	Shiny black
Radiation	Mo$K\alpha$ ($\lambda = 0.71073$ Å)	Mo$K\alpha$ ($\lambda = 0.71073$ Å)
	Graphite monochromated	Graphite monochromated
μ(Mo$K\alpha$) (cm^{-1})	361.4	437.8
Scan mode	ω	ω
Scan width (°)	1.40	1.40
Range measured	$3° \le 2\theta \le 80°$	$3° \le 2\theta \le 70°$
	$-9 \le h \le 9$	$-10 \le h \le 10$
	$-10 \le k \le 10$	$0 \le k \le 16$
	$-15 \le 1 \le 15$	$-20 \le 1 \le 20$
Period of intensity control	100 reflections	100 reflections
Measured reflections	5004	6132
Independent reflections	5004	3086
Internal consistency factor		0.067
Absorption correction	Psi scan	Psi scan
Observed reflections ($F > 4\sigma(F)$)	4142	2337
Structure determination	Patterson method	Direct method
Refinement (16)	SHELXL-93	SHELXL-93
Parameters refined	107	170
Weighting scheme	$w^{-1}(F^2) = \sigma^2(F^2) + (0.035F^2)^2$	$w^{-1}(F^2) = \sigma^2(F^2) + (0.03F^2)^2$
Residuals	$R = 0.049$ on F	$R = 0.040$ on F
	w$R2 = 0.107$ on F^2	w$R2 = 0.086$ on F^2

TABLE 3
Positional and Thermal Parameters of $PtSi_3P_2$

Atom	Position	x/a	y/b	z/c	u_{eq}
Pt1	1a	0	0	0	0.0086(1)
Pt2	1a	0.8522(1)	0.71571(8)	0.55837(6)	0.0080(1)
Si1	1a	0.665(1)	0.966(1)	0.7548(7)	0.0084(8)
Si2	1a	0.565(1)	0.332(1)	0.6686(8)	0.0109(9)
Si3	1a	0.350(1)	0.023(1)	0.2311(8)	0.0099(9)
Si4	1a	0.053(1)	0.450(1)	0.3984(7)	0.0095(8)
Si5	1a	0.671(1)	0.609(1)	0.0751(8)	0.0102(8)
Si6	1a	0.180(1)	0.756(1)	0.8053(8)	0.0107(9)
P1	1a	0.493(1)	0.691(1)	0.3173(7)	0.0096(7)
P2	1a	0.795(1)	0.268(1)	0.1627(7)	0.0098(7)
P3	1a	0.298(1)	0.397(1)	0.8853(7)	0.0099(7)
P4	1a	0.190(1)	0.118(1)	0.4807(1)	0.0107(7)

tetrahedra with Pt atoms at vertices are not occupied independent polyhedra. These tetrahedra overlap with octahedra, while one, two, or three of their corners are located at the center of one, two, or three octahedra. The differences in the atomic arrangements of these compounds are reflected in the different ways in which the M(Si/P)$_6$ octahedra are linked via common corners or/and edges.

The $PtSi_3P_2$ structure can be described by two crystallographically independent Pt1 and Pt2 octahedra connected pairwise by edge-sharing. The resulting $Pt_2(Si/P)_{10}$ double octahedron constitutes the crystal structure pattern (Fig. 1). On both sides of the Si1–Si6 common edge, each Pt atom is surrounded by two phosphorus and two silicon atoms. Si and P atoms are tetrahedrally coordinated: one or two Pt atoms are located on vertices of each tetrahedron. In principle, metal–metal bonding could occur when octahedra are

TABLE 4
Positional and Thermal Parameters of $PtSi_2P_2$

Atom	Position	x/a	y/b	z/c	u_{eq}
Pt1	2*a*	0.8957(1)	0.03154(5)	0.62563(6)	0.0120(2)
Pt2	2*a*	0.4047(1)	0.34799(6)	0.64142(6)	0.0117(1)
Pt3	2*a*	0.0912(1)	0.70499(5)	0.86012(6)	0.0078(2)
Pt4	2*a*	0.3932(1)	0.51786(5)	0.12709(6)	0.0071(1)
Si1	2*a*	0.0504(9)	0.4542(5)	0.1763(4)	0.0117(9)
Si2	2*a*	0.4619(9)	0.7911(7)	0.8325(5)	0.0137(7)
Si3	2*a*	0.2669(9)	0.3088(4)	0.4336(7)	0.0085(9)
Si4	2*a*	0.0251(1)	0.0825(6)	0.9184(4)	0.014(1)
Si5	2*a*	0.2367(8)	0.5694(5)	0.5801(4)	0.0079(5)
Si6	2*a*	0.956(1)	0.6264(8)	0.6669(6)	0.016(1)
Si7	2*a*	0.435(1)	0.7749(8)	0.6410(6)	0.018(1)
Si8	2*a*	0.5466(8)	0.4214(4)	0.8371(8)	0.006(1)
P1	2*a*	0.0667(7)	0.2916(4)	0.8591(3)	0.011(1)
P2	2*a*	0.243(1)	0.7472(7)	0.0656(5)	0.016(1)
P3	2*a*	0.766(1)	0.4360(6)	0.6104(4)	0.017(1)
P4	2*a*	0.466(1)	0.6109(5)	0.3241(5)	0.0086(7)
P5	2*a*	0.041(1)	0.2718(4)	0.6680(5)	0.010(1)
P6	2*a*	0.2487(9)	0.9627(6)	0.5855(5)	0.0092(9)
P7	2*a*	0.7409(8)	0.6285(5)	0.8977(4)	0.0078(8)
P8	2*a*	0.736(1)	0.9755(6)	0.0709(5)	0.0119(9)

paired with one common edge as in MnP_4 (11), but the distortions of Pt octahedra are such that in a double octahedron, the metal atoms remain widely separate (Pt–Pt = 3.77 Å). Two neighboring double octahedra have no common corner; they are linked to each other only by bonds between nonmetal atoms (–Si/P–Si/P–).

The $PtSi_2P_2$ crystal structure pattern can be described by a cluster of four edge-sharing platinum octahedra Pt1, Pt2,

TABLE 5
Bond Lengths and Angles Observed in Occupied Polyhedra of $PtSi_3P_2$

Pt1–	Distance	Angles				
Si5	2.356(5)					
Si6	2.404(7)	88.1(2)				
Si3	2.413(6)	94.3(2)	97.9(2)			
P2	2.414(6)	94.9(2)	172.2(2)	89.0(2)		
Si1	2.442(6)	86.3(2)	78.4(2)	176.3(2)	94.6(2)	
P3	2.450(5)	171.9(2)	89.5(2)	93.7(2)	86.5(2)	85.6(2)
	Pt1	Si5	Si6	Si3	P2	Si1
Pt2–	Distance	Angles				
Si2	2.360(5)					
Si4	2.378(6)	86.3(2)				
Si6	2.426(7)	85.8(2)	95.9(2)			
P4	2.425(5)	172.1(2)	95.2(2)	86.3(2)		
Si1	2.457(6)	89.7(2)	172.7(2)	77.7(2)	87.9(2)	
P1	2.497(6)	93.80(2)	88.5(2)	175.5(2)	93.9(2)	97.8(2)
	Pt2	Si2	Si4	Si6	P4	Si1

TABLE 6
Bond Lengths and Angles Observed in Occupied Polyhedra of $PtSi_2P_2$

Pt2–	Distance	Angles				
Si3	2.365(5)					
P6	2.372(6)	91.4(2)				
Si1	2.422(4)	88.7(2)	100.4(2)			
Si5	2.429(4)	79.0(2)	86.8(2)	165.9(2)		
P5	2.449(4)	174.0(2)	90.1(2)	96.6(2)	95.3(2)	
P4	2.500(6)	90.8(2)	177.2(2)	78.0(2)	95.1(2)	87.8(2)
	Pt1	Si3	P2	Si1	Si5	P5
Pt2–	Distance	Angles				
Si5	2.371(5)					
P4	2.381(5)	170.8(2)				
P5	2.394(6)	88.1(2)	88.1(2)			
Si8	2.399(4)	94.5(2)	94.2(2)	95.5(2)		
P3	2.435(6)	89.2(2)	94.5(2)	177.2(2)	84.9(2)	
Si3	2.457(5)	78.3(2)	93.1(2)	88.5(2)	171.6(2)	90.6(2)
	Pt2	Si5	P4	P5	Si8	P3
Pt3–	Distance	Angles				
P7	2.367(5)					
Si6	2.382(7)	87.7(2)				
P2	2.447(6)	90.6(2)	171.1(2)			
P8	2.468(5)	89.6(2)	94.2(2)	77.0(2)		
Si2	2.467(6)	176.5(2)	95.7(2)	86.0(2)	90.5(2)	
Si1	2.514(5)	92.1(2)	95.5(2)	93.2(2)	170.1(2)	87.1(2)
	Pt3	P7	Si6	P2	P8	Si2
Pt4–	Distance	Angles				
Si2	2.326(6)					
P8	2.347(5)	94.3(2)				
Si1	2.348(5)	91.2(2)	95.3(2)			
Si4	2.402(6)	88.2(2)	85.9(2)	178.6(2)		
P2	2.402(7)	174.2(2)	80.2(2)	90.9(2)	89.6(2)	
P4	2.453(6)	98.8(2)	166.1(2)	80.3(2)	98.4(2)	86.6(2)
	Pt4	Si2	P8	Si1	Si4	P2
Si7–	Distance	Angles				
P6	2.127(9)					
Si3	2.198(9)	100.0(3)				
Si2	2.256(9)	99.8(4)	121.2(4)			
Si5	2.312(9)	114.0(4)	114.1(4)	106.9(3)		
	Si7	P6	Si3	Si2		
P1–	Distance	Angles				
P8	2.166(7)					
P5	2.255(6)	111.3(3)				
P2	2.284(8)	115.0(3)	120.2(3)			
Si4	2.303(6)	112.8(3)	99.0(2)	95.9(3)		
	P1	P8	P5	P2		

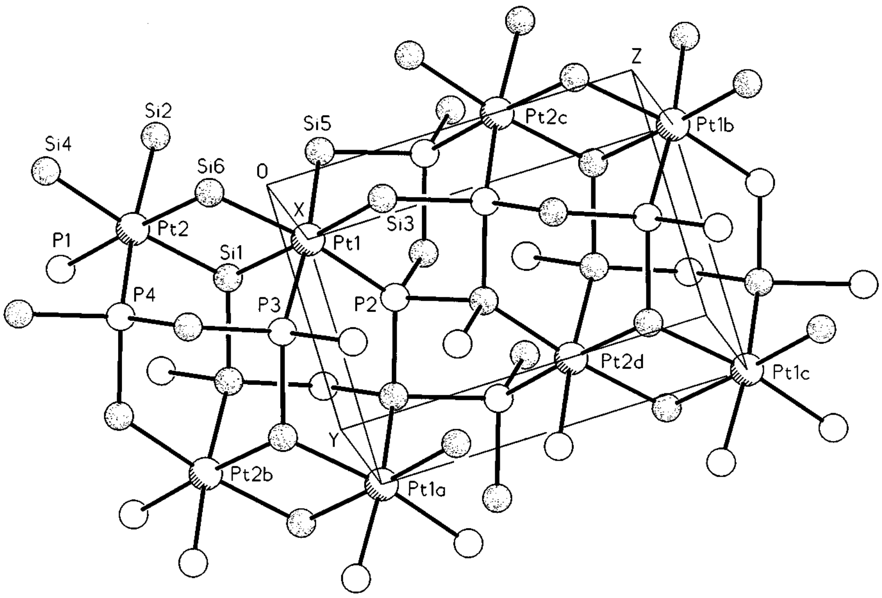

FIG. 1. Crystal structure of $PtSi_3P_2$ viewed along the [100] direction.

Pt3, and Pt4 and by two tetrahedra P1 and Si7 (Fig. 2). Each Pt atom is surrounded by six nonmetal atoms: three silicium and three phosphorus atoms. No metal–metal bonding occurs (shortest Pt–Pt = 3.70 Å). Tetrahedra P1 and Si7 are surrounded by nonmetal atoms: P1 has three neighbors P and one neighbor Si; Si7 has three neighbors Si and one neighbor P. As in $CoSi_3P_3$, the Si7 tetrahedron is smaller ($\langle$Si7–P/SI$\rangle$ = 2.223 Å) than the P1 tetrahedron ($\langle$P1–Si/P$\rangle$ = 2.252 Å). On the whole, tetrahedra differ from these of $PtSi_3P_2$; as a matter of fact they can be completely nonmetallic (P1 and Si7), Si1 and P4 atoms are common corners of three octahedra; the Si1 and P4 tetrahedra then have three Pt vertices. Moreover, while octahedra couples are separated from each other in the $PtSi_3P_2$ structure, two neighboring clusters are linked by one common corner (Si1 or P4), and the completely nonmetallic tetrahedra P1 and Si7 establish bonding between four clusters (Fig. 3).

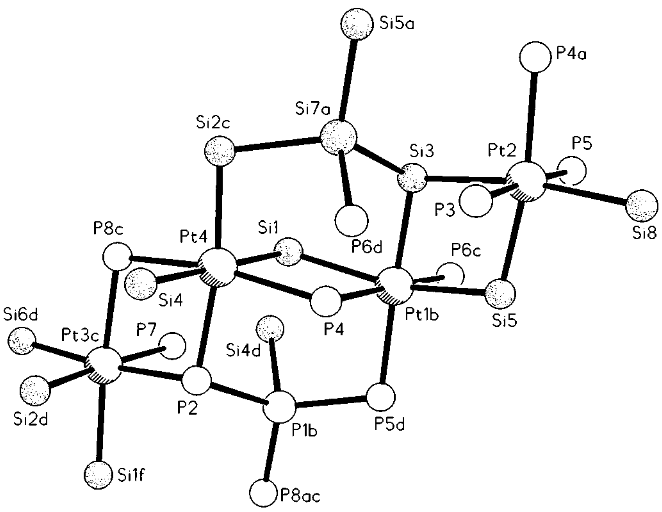

FIG. 2. Crystallographic pattern of $PtSi_2P_2$.

ELECTRICAL RESISTIVITY

$PtSi_2P_2$ crystals are very hygroscopic; it was impossible to measure the resistivity by the four contacts method. Figure 4 presents the resistivity of $PtSi_3P_2$ single crystal between 4.2 K and 300 K. Because of the not very well defined sample shape, the absolute precision of the resistivity values is only about 20%. In he whole temperature range the resistivity increases with temperature but this variation is quite small, only about 20%. The curve exhibits two regimes: above 50 K, ρ increases linearly with T and below this temperature, ρ follows a somewhat higher power law. It is, however, not possible to assimilate this behavior to a metallic one as the absolute resistivity values are quite high (some mΩ cm), and at lowest temperature no constant residual resistivity can be observed in a significant temperature range, as expected for a metal. More detailed investigations are necessary to unambiguously classify the electrical behavior of $PtSi_3P_2$.

CONCLUSION

New ternary nonmetal-rich compounds $M\mathrm{Si}_x\mathrm{P}_y$ with $M = \mathrm{Pt}$ have been synthetized. As for the previously

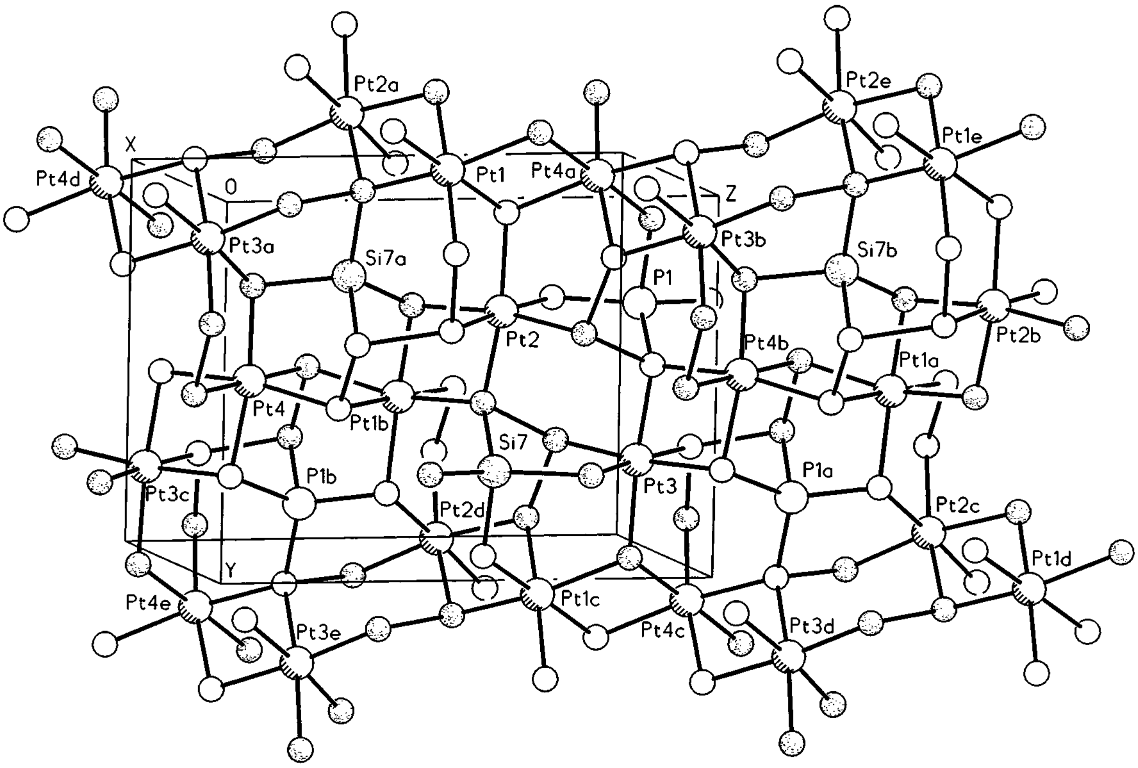

FIG. 3. Crystal structure of $PtSi_2P_2$ viewed along the [100] direction.

reported MSi_4P_4, MSi_3P_3, and MSi_3P_4 phases, the crystal structure of the new platinum phosphosilicides crystallizes in acentric space groups: $P1$ for $PtSi_3P_2$ and $P2_1$ for $PtSi_2P_2$; Pt and Si/P atoms are respectively octahedrally and tetrahedrally coordinated. The two crystal structures show many similarities in their descriptions which only differ by the way of condensing platinum octahedra.

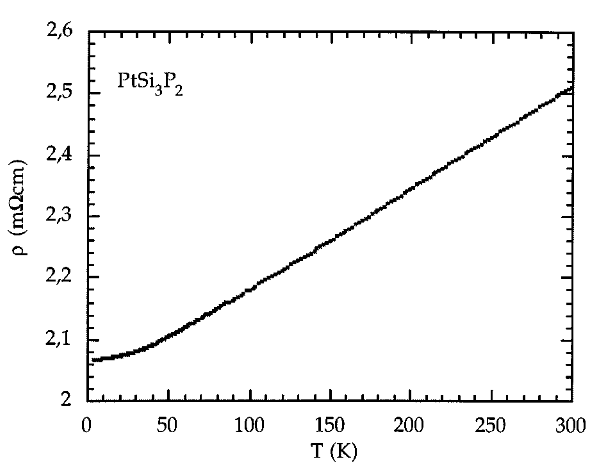

FIG. 4. Electrical resistivity of the $PtSi_3P_2$ single crystal.

REFERENCES

1. R. Gohle and K. Schubert, *Z. Metallkde.* **55,** 503 (1964).
2. B. Y. Tsaur and J. W. Mayer, *J. Appl. Phys.* **51**(10), 5326 (1980).
3. A. Baghdadi, A. Finley, P. Russo, R. J. Arnott, and A. Wold, *J. Less-Common Metals* **34,** 31 (1974).
4. O. G. Folberth and H. Pfister, *Acta crystallogr.* **14,** 325 (1961).
5. R. Vogel and B. Giessen, *Arch. Eisenhüttenw.* **30,** 619 (1959).
6. O. N. Il'Nitskaya and Yu. B. Kuz'ma, *Izv. Akad. Nauk SSSR, Met.*, 215 (1992).
7. O. N. Il'Nitskaya, V. A. Bruskov, P. Yu. Zavalii, and Yu. B. Kuz'ma, *Izv. Akad. Nauk SSSR, Neorg. Mater.* **27**(6), 1311 (1991).
8. O. N. Il'Nitskaya, P. Yu. Zavalii, and Yu. B. Kuz'ma, *Dopov. Akad. Nauk Ukr. RSR, Ser. B*, 38 (1989).
9. H. Vincent, Ch. Perrier, M. Kirschen, P. Chaudouet, and R. Madar, "11th ICSCTE, International Conference on Solid Compounds of Transition Elements." Wrocław, Poland, 1994.
10. Ch. Perrier, Thesis, Institut National Polytechnique de Grenoble, France, 1995.
11. Ch. Perrier, H. Vincent, P. Chaudouët, B. Chenevier, and R. Madar, *Mat. Res. Bull.* **30**(3), 357 (1995).
12. M. Kirschen, H. Vincent, Ch. Perrier, P. Chaudouët, B. Chenevier, and R. Madar, *Mat. Res. Bull.* **30**(4), 507 (1995).
13. J. Kreisel, O. Chaix-Pluchery, F. Genet, G. Lucazeau, H. Vincent, and R. Madar, *J. Solid State Chem.* **128,** 142 (1997).
14. H. Vincent, J. Kreisel, Ch. Perrier, O. Chaix-Pluchery, P. Chaudouët, and R. Madar, *J. Solid State. Chem.* **124,** 366 (1996).
15. J. Wallinda and W. Jeitschko, *J. Solid State Chem.* **114,** 476 (1995).
16. G. Sheldrick, "SHELXL-93." Institut Anorganischer Chemie, Göttingen, 1993.